

A high-performance EMI filter based on laminated ferrite ring cores

Marcin Kącki¹, Marek S. Rylko¹, John G. Hayes², Charles R. Sullivan³

¹ Research and Development SMA Magnetics Sp. z o.o.
Modlniczka, Poland

e-mail: marcin.kacki@sma-magnetics.com / marek.rylko@sma-magnetics.com

² Power Electronics Research Laboratory School of Engineering University College Cork
Cork, Ireland

e-mail: john.hayes@ucc.ie

³ Thayer School of Engineering Dartmouth College
Hanover, NH 03755, USA
e-mail: charles.r.sullivan@dartmouth.edu

Keywords

EMC/EMI, Passive filters, Ferrite, Optimization

Abstract

This paper presents a study on the flux distribution and impedance of common-mode chokes based on the solid and laminated ferrite ring cores. The analysis demonstrates the novel laminated core structure to improve the flux distribution across the core cross-section at high frequency, and so, also improves the overall EMI filter performance. Solid and laminated ferrite common-mode chokes are implemented in a two-stage single-phase EMI filter and compared experimentally.

Introduction

The continuous drive for improvement of energy conversion focuses on efficiency improvement combined with switching frequency increases, which result in size and cost reductions. This leads to new solutions and is fostering an interest in the wide-bandgap (WBG) silicon carbide (SiC) and gallium nitride (GaN) semiconductors, which have superior switching performance in comparison to the traditional Silicon (Si) based power semiconductors. The benefits of using such semiconductors, i.e., higher switching frequencies, higher rate of voltage (dv/dt) and current (di/dt) transients, and higher power density, create a new frontier for EMI filtering and magnetic component design. EMI generation is strongly related to the rate of voltage (dv/dt) transients and their frequencies. In order to compare EMI footprints, three spectra are compared to demonstrate the effect of switching frequency and fast voltage (dv/dt) transients. The EMI emission spectra for Si, SiC and GaN are shown in Fig. 1. The spectra are the Fourier analysis of trapezoidal switching signals with parameters as listed in Table I. The operating frequency of the semiconductors is taken as a most common for the respective type of semiconductors [1]-[6].

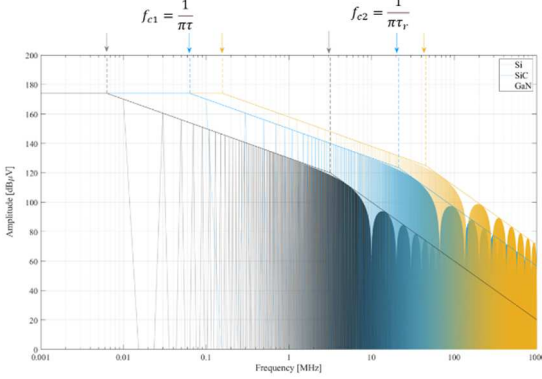


Fig. 1: EMI emission spectra for Si (black), SiC (blue) and GaN (orange).

Table I: Trapezoidal signal parameters

	Unit	Si	SiC	GaN
Amplitude	V	500	500	500
Switching Frequency	kHz	10	100	250
Rise/fall time	ns	100	15	8
$\tau_r = \tau_f$				

Application of WBG semiconductors allow for operation with higher frequencies, and thus, the EMI envelope is shifted to higher frequencies, which is challenging for magnetic component design. Effects that are otherwise negligible become significant, such as skin depth and dimensional resonance. The higher influence of filter parasitics and couplings must be addressed with specific models and more advanced designs to provide high-performance EMI filter designs. A laminated Mn-Zn ferrite ring core is proposed to improve the flux distribution, the core frequency characteristics, and the overall EMI filter performance, which is reduced by the skin and dimensional resonance effects in traditional designs. It has been known for over a century that laminating eliminates eddy-current losses in iron-based cores. Eddy-current losses in laminated cores are reduced by a factor $1/n^2$, where n is the number of laminations, as the path of the induced electric field is closed in each lamination [7][8]. However, ferrite is perceived as a high-impedance bulk body. However, the ferrite structure may develop conductive paths in certain conditions. Additionally, the ferrite core lamination helps to reduce one of the core cross-sectional dimensions, and therefore the frequency at which the dimensional resonance occurs can be significantly increased. FEA simulations were performed to quantify the effect of laminating on the flux distribution in the ferrite ring core. The FEA calculation uses a 3-D eddy-current field solver. The simulation results are shown in Fig. 3. Intuitively, in the solid core cross-section the magnetic flux is concentrated in the outer circumference, while the core center exhibits flux density weakening due to the skin effect. The laminated core, on the other hand, shows only a relatively marginal magnetic field change [9]-[12], with a resulting improvement in flux distribution and utilization.



Fig. 2: Ferrite eddy current reduction with lamination.

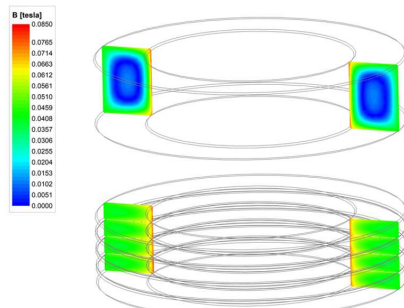


Fig. 3: FEA results of flux distribution in the solid and laminated ferrite ring core.

Core size and material selection effect on lamination

The laminated core structure divides the conduction path into sub-regions that reduce the high-frequency effects. For such structures, the upper end of the frequency range is limited by the minimum lamination size. The feasible lamination thickness directly impacts the core's complex characteristic at high

frequencies. Thin laminations shift the skin and dimensional resonance effects to higher frequencies. In order to investigate how lamination performance depends on core size and material, we compare the complex permeability characteristics for three bulk core sizes, T29, T50, and T80, made of two materials, 3F36 and 3E10. The laminated cores are stacked together from smaller cores with a thickness of 3.5 mm. The T29 laminated core is stacked out of 3 laminations, while the T50 out of 4, and the T80 out of 5 laminations. Table II shows the cores parameters used for this test.

Table II: Core parameters used for the tests

Core type	Core material	Dimensions OD x ID x H	Core cross section dimension	Core cross section	Core volume
Unit	-	mm	mm	mm ²	cm ³
T29 Solid	3F36/3E10	29 x 19 x 10.5	5 x 10.5	53	3.96
T29 Laminated	3F36/3E10	29 x 19 x 3.5 x 3	5 x 3.5 x 3	53	3.96
T50 Solid	3F36/3E10	50 x 30 x 14	10 x 14	140	17.59
T50 Laminated	3F36/3E10	50 x 30 x 3.5 x 4	10 x 3.5 x 4	140	17.59
T80 Solid	3F36/3E10	80 x 45 x 17.5	17.5 x 17.5	306	60.13
T80 Laminated	3F36/3E10	80 x 45 x 3.5 x 5	17.5 x 3.5 x 5	306	60.13



The measured complex frequency characteristics are presented in Fig. 4 and Fig. 5 for the 3F36 material, and in Fig. 6 and Fig. 7 for the 3E10 material. Since the core size varies it requires a customized measurement fixture. Construction of the fixture provides one turn equally distributed around the toroidal core specimen. The fixture is in the shape of a cylindrical cup which forms a short-ended coaxial line over the tested core. This measurement method provides accurate results and allows for measurement up to 1 GHz. Measurements are performed with a Wayne Kerr 6550B analyzer.

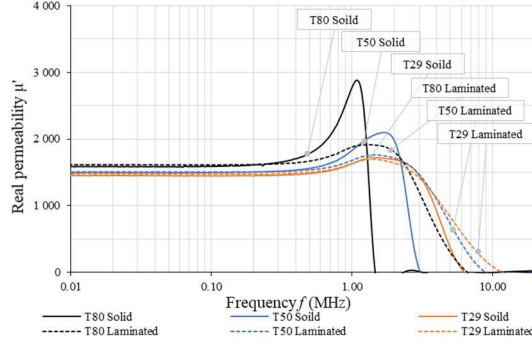


Fig. 4: 3F36 ferrite real permeability vs. frequency for various core sizes.

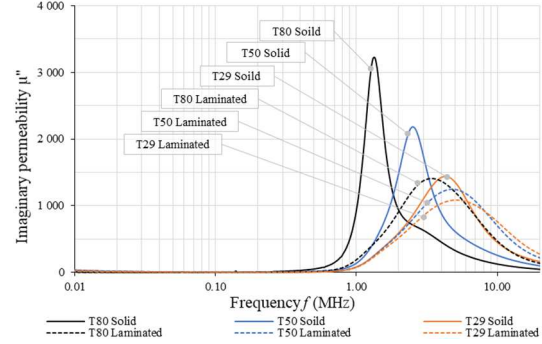


Fig. 5: 3F36 ferrite imaginary permeability vs. frequency for various core sizes.

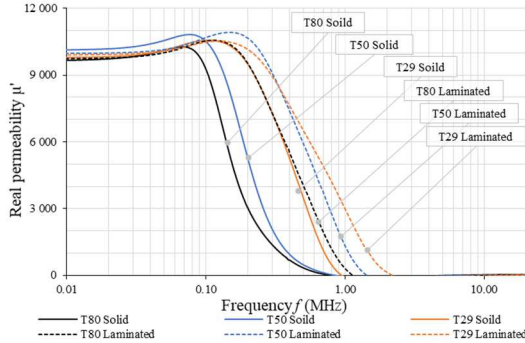


Fig. 6: 3E10 ferrite real permeability vs. frequency for various core sizes.

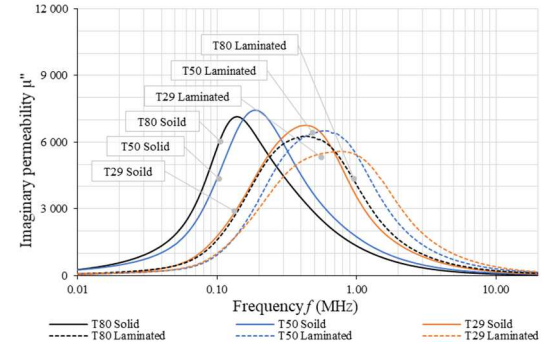


Fig. 7: 3E10 ferrite imaginary permeability vs. frequency for various core sizes.

As can be observed, the laminated cores, regardless of their size and material, show significant improvements in the frequency characteristic. The laminated T80 core maintains its performance up to 6 MHz for the 3F36 material, exactly the same as the smaller T29 solid core. The measured real permeability characteristic for the T29 bulk core, made of the 3F36 material, drops to zero at 6 MHz, while the laminated core keeps its characteristic up to 11 MHz. The biggest improvement in the imaginary permeability characteristic is visible in the T80 core. A significant loss increase, visible in the 3F36 material and caused by dimensional resonance, is reduced by half, and shifted to higher frequencies. Improvement is also visible in high permeability materials such as 3E10. The real permeability characteristic is extended from 1 MHz to 2 MHz, while the loss peak of the imaginary permeability characteristic for the T80 is reduced by 60%.

Single-phase EMC filter based on the laminated ferrite core

In order to show the differences between the solid and laminated cores in a potential application, four single-phase common-mode chokes are built. The basic construction parameters for the designed chokes are presented in Table III. The construction details are the identical for all the chokes, except for the core. The turns are wound in single layers to reduce the winding effects on the impedance characteristic

Table III: Common mode choke parameters

Parameter	Unit	Sample 1/ Sample 2	Sample 3/ Sample 4
Core material	-	Mn-Zn ferrite	Mn-Zn ferrite
Core dimensions OD x ID x H	mm	50 x 30 x 14	50 x 30 x 2.8 x 5 5 laminations
Material perm.	-	12 000	12 000
Number of turns	-	8/phase	8/phase
Wire type	-	1.8 mm Cu wire	1.8 mm Cu wire
CM Inductance	mH	1.19 / 1.15	1.05 / 1.11
Rated current	A	20	20

The measured choke inductance and impedance frequency characteristics are shown in Fig. 8 and Fig. 9, respectively. The laminated CM choke in comparison to the solid core has improved its performance in the frequency range between 200 kHz and 20 MHz. Compared to the CMC based on solid cores, the laminated choke impedance is doubled in the frequency range between 1 MHz and 20 MHz, while both chokes have the same size.

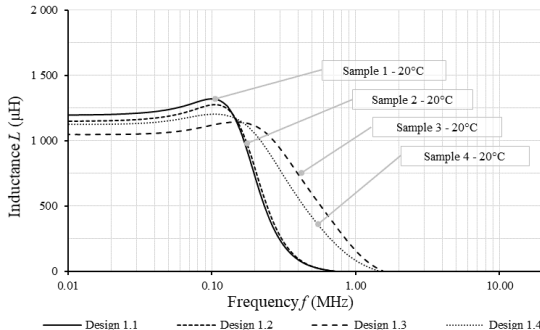


Fig. 8: Tested CMC inductance vs. frequency.

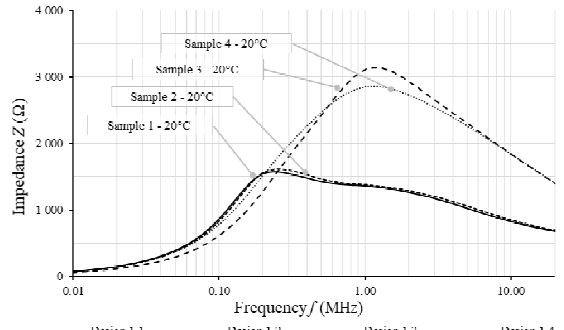


Fig. 9: Tested CMC impedance vs. frequency.

As a final step, the designed common mode chokes are integrated into the two-stage EMI filter to demonstrate the laminated core advantages in the filter structure. The EMI filter schematic is shown in Fig. 10, while the list of components is presented in Table IV.

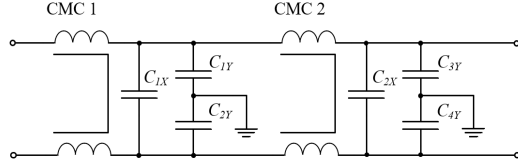


Fig. 10: Schematic of the two-stage EMI filter.

Table IV: EMI filter components

Component	Description
CMC – solid core	Design 1.1 and Design 1.2
CMC – laminated core	Design 1.3 and Design 1.4
Capacitor C _{1X}	4.7µF - Kemet F863RL475M310ALW0L
Capacitor C _{2X}	2.2µF - Kemet F863FL225MK310ALW0L
Capacitor C _{1Y} , C _{2Y} , C _{3Y} , C _{4Y} ,	22nF - Epcos B32022A3223M

A photo of the tested EMI filters is shown in Fig. 11. Both PCBs used for the comparison are identical. The measured common-mode insertion loss characteristic for the two EMI filters is shown in Fig. 12. The evaluation shows that the proposed laminated ferrite structure provides significant attenuation improvement in the frequency range between 200 kHz and 20 MHz. Above 1 MHz, the difference is about 10 dB, while both filters maintain the same size.



Fig. 11: Complete EMI filters for CMC test.

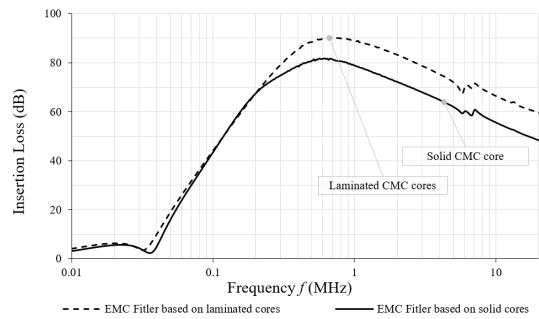


Fig. 12: EMI filters common-mode insertion loss.

Conclusion

Ferrite magnetic materials are subject to high-frequency effects which result in non-uniform frequency-dependent magnetic flux distributions. Laminated cores open up new horizons for EMI filter design. The proposed core structure can overcome the poor flux distribution caused by skin and dimensional-resonance effects. Laminated Mn-Zn ferrite ring cores show a significant improvement in the flux distribution resulting in improved frequency characteristics.

References

- [1] E. Hoene, G. Deboy, C.R. Sullivan, G. Hurley, "Outlook on developments in power devices and integration: recent investigations and future requirements," *IEEE Power Electronics Magazine*, vol. 5, March 2018.
- [2] J. Millan, P. Godignon, X. Perpina, A. Perez-Tomas, J. Rebollo, "A survey of wide bandgap power semiconductors devices," *IEEE Trans. Power Electron.*, vol.29 no.5 pp.2155-2163, 2014.
- [3] J. Biela, M. Schweizer, S. Waffler, B. Wrzecionko, J.W. Kolar, "SiC vs. Si evaluation of potentials for performance improvement of power electronics converter system by SiC power semiconductors," *Industrial Electronics, IEEE Transactions*, vol. 58, issue 7, pp. 2872–2882, July 2011.

- [4] Di Han, J. Noppakunkajorn, B. Sarlioglu, "Comprehensive Efficiency, Weight, and Volume Comparison of SiC- and Si-Based Bidirectional DC–DC Converters for Hybrid Electric Vehicles," *IEEE Transactions on Vehicular Technology*, vol. 63, issue: 7, September 2014.
- [5] J.W. Kolar, J.E. Huber, "Future Power Electronics 4.0 3-Phase SiC/GaN Converter Systems," *Tutorial at the 36th Applied Power Electronics Conference and Exposition (APEC2021)*, June 2021
- [6] N. Oswald, B.H. Stark, D. Holliday, C. Hargis, "Analysis of shaped pulse transitions in power electronics switching waveforms for reduced EMI," *IEEE Transactions on Industry Application*, vol. 47, issue: 5, October 2011.
- [7] D.J. Griffiths, "Instruction to Electrodynamics" Price Hall, 1999.
- [8] E.C. Snelling, Soft ferrites: properties and applications, Newnes-Butterworth; 1St Edition, 1969
- [9] G.R. Skutt, "High-frequency dimensional effects in ferrite-core magnetic devices," Ph.D. dissertation, Virginia Polytechnic Institute, Blacksburg, Virginia, 1996
- [10] G.R. Skutt, F.C. Lee, "Characterization of dimensional effects in ferrite-core magnetic devices," *IEEE Power Electronics Specialist Conference*, Jun. 1996
- [11] M. Kącki, M.S. Ryłko, J.G Hayes, C.R. Sullivan, "Magnetic material selection for EMI filter," *IEEE Energy Conversion Congress and Exposition (ECCE)*, October 2017.
- [12] M. Kącki, M.S. Ryłko, J.G Hayes, C.R. Sullivan, "A study of flux distribution and impedance in solid and laminar ferrite cores," *IEEE Applied Power Electronics Conference and Exposition (APEC)*, March 2019.